Organic & Biomolecular Chemistry

RSC Publishing

PAPER

View Article Online
View Journal | View Issue

Cite this: *Org. Biomol. Chem.*, 2013, **11**, 318

Self-decarboxylation of trichloroacetic acid redox catalyzed by trichloroacetate ions in acetonitrile solutions†

Drochss P. Valencia,[a] Pablo D. Astudillo,[a] Annia Galano[b] and Felipe J. González*[a]

Received 8th October 2012,
Accepted 30th October 2012

DOI: 10.1039/c2ob26961a

www.rsc.org/obc

In mixtures of trichloroacetate ion and trichloroacetic acid in acetonitrile, trichloromethyl radicals are produced as a result of the redox reaction between the acid and its conjugate base. The reaction follows a loop mechanism in which the trichloroacetic acid is slowly consumed by proton reduction while the trichloroacetate ion is oxidized like in an electrochemical Kolbe reaction. The hydroquinone–trichloroacetate complex was a good sensor of this unexpected self-decarboxylation redox reaction.

Introduction

The anodic oxidation of carboxylates ($RCOO^-$) is an old reaction that allows the synthesis of a great variety of products derived from radical or carbocation chemistry (Scheme 1).[1] The radical pathway (Kolbe reaction) is mainly focused on the synthesis of symmetric and unsymmetric dimers and radical coupling products derived from addition to double bonds. Alternatively, depending on the electrolysis conditions, the carbocation pathway (non-Kolbe reaction) can be triggered to prepare products derived from reactions with nucleophilic species, which allow the formation of compounds such as alcohols, ethers, esters, acetamides *etc.* More recently the covalent grafting of organic moieties on carbon surfaces by direct and mediated oxidation of carboxylates has also been considered between the main applications of the carboxylate oxidation reaction.[2]

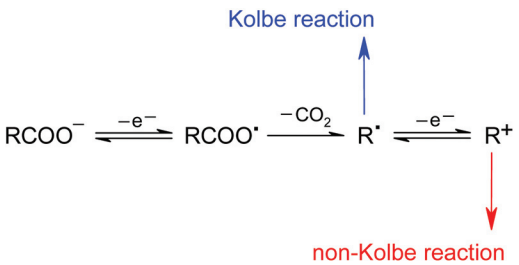

Scheme 1 Electrochemical oxidation of carboxylates.

Although most of the mechanistic studies of this reaction were based on the analysis of electrolysis products, recent studies indicate that the first electron transfer uptake gives rise to a transient acyloxy radical ($RCOO^{\bullet}$) which is immediately decomposed into a free radical ($R^{\bullet}$) and carbon dioxide.[3] Due to the instability of acyloxy radicals,[4] and the high stability of both carbon dioxide and the products of the radical and/or carbocation coupling, the decarboxylation reaction represents an important driving force of either the Kolbe or non-Kolbe overall mechanisms. In this framework, it can be proposed that the interaction between carboxylates and molecules having the ability to gain electrons through a redox reaction represents a good option to initiate chemically any of the reaction pathways mentioned above.

On the other hand, it is well known that the acidity of carboxylic acids is sensitive to the presence of substituents in the molecular structure of the acid. Thus, electron-releasing groups contribute to decrease the acidity while electron-withdrawing groups contribute to increase this property. From the electrochemical point of view, the presence of substituents in the acid structure is also manifested through differences in the reduction potential of the acidic proton, such as was demonstrated in some studies about the reduction of organic compounds possessing acidic functional groups on platinum electrodes.[5] In this way, the higher is the acidity of the acid, the lower is its reduction potential.

Considering both the oxidation features of carboxylates and the redox reduction features of the acidic proton of the corresponding acids, in this work it is proposed that mixtures of carboxylates derived from strong carboxylic acids can be involved in an intermolecular electron transfer reaction leading to an overall self-decarboxylation process. In order to

[a]*Departamento de Química del Centro de Investigación y de Estudios Avanzados del I.P.N., Av. IPN 2508, Col. San Pedro Zacatenco, 07360 Distrito Federal, Mexico. E-mail: fgonzale@cinvestav.mx; Fax: +52 55 57477113; Tel: +52 55 57473728*
[b]*Departamento de Química de la Universidad Autónoma Metropolitana-Iztapalapa, San Rafael Atlixco 186, Col. Vicentina, 09340 Distrito Federal, Mexico*
†Electronic supplementary information (ESI) available. See DOI: 10.1039/c2ob26961a

demonstrate this hypothesis the behaviour of mixtures of trichloroacetate ions (Cl_3CCOO^-) and trichloroacetic acid (Cl_3CCOOH) in acetonitrile was analysed by cyclic voltammetry, spectroscopy and theoretical calculations to evaluate the electron exchange between these two species.

The fundamental aspects of the problem analyzed here are of relevance to the understanding of the mechanisms of decomposition of haloacetic acids, which are found between the main halogenation products of drinking water.[6]

Results and discussion

The origin of the problem here discussed arises from a preliminary study about the two-electron reduction of 1,4-benzoquinone (Q) in the presence of proton donors such as trichloroacetic acid (Cl_3CCOOH) in acetonitrile. The overall reaction stoichiometry of this electrochemical reaction shows that hydroquinone (QH_2) and trichloroacetate ions (Cl_3CCOO^-) are formed in a 1 : 2 molar ratio (eqn (1)).

$$Q + 2e^- + 2Cl_3CCOOH = QH_2 + 2Cl_3CCOO^- \quad (1)$$

This process presents a typical voltammetric pattern which is shown in Fig. 1. Curve "A" corresponds to the behaviour of the 1,4-benzoquinone in the absence of Cl_3CCOOH. In this figure, peaks Ic–Ia and IIc–IIa correspond respectively to the quinone/semiquinone ($Q/Q^{\cdot -}$) and the semiquinone/dianion ($Q^{\cdot -}/Q^{2-}$) reversible redox couples.[7] On the other hand, when an excess of Cl_3CCOOH is added to the solution of 1,4-benzoquinone, the curve "B" is obtained. Under these conditions, the chemically irreversible peak IIIc is related to the two-electron global process depicted by eqn (1), while the oxidation peak IIIa is related to the oxidation of a hydrogen bonding association complex between hydroquinone and trichloroacetate ions. The 1 : 2 complex is yellow and its anodic peak potential at a scan rate of 0.1 V s^{-1} (0.695 V/SCE) is lower than that of pure hydroquinone (0.982 V/SCE) (curve "C", peak IVa).

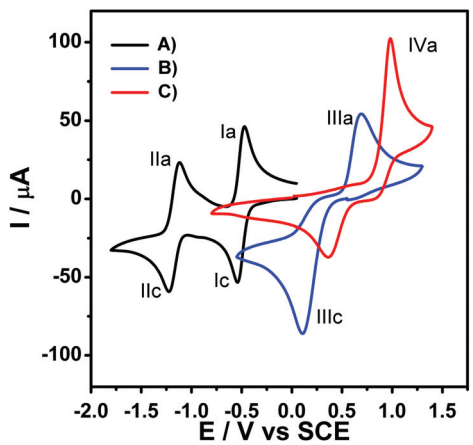

Fig. 1 Cyclic voltammetry in acetonitrile +0.1 M n-Bu_4NPF_6 on a glassy carbon electrode (3 mm diameter) at 0.1 V s^{-1}. (A) 1,4-benzoquinone 2 mM; (B) 1,4-benzoquinone 2 mM + HTCA 20 mM; (C) hydroquinone 2 mM.

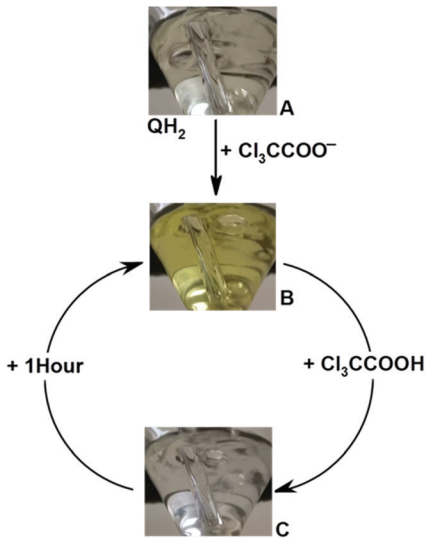

Scheme 2 The hydroquinone as a chemical sensor.

Under the experimental conditions of Fig. 1B, the reaction stoichiometry is described by eqn (1), the excess of HTCA determining potential peak IIIa. Until now, the results described above have been satisfactorily understood from previous work,[8] however, several problems of solution instability were found when the mixture $QH_2 : Cl_3CCOO^- : Cl_3CCOOH$ (2 : 4 : 20) was prepared in order to emulate approximately the interfacial conditions existing at the beginning of oxidation of the association complex during the reverse scan of curve "B" (peak IIIa). The problems here suggested can be described in terms of Scheme 2, which shows several pictures of the electrochemical cell under different conditions of chemical composition.

Scheme 2A shows the appearance of the initial colourless solution of hydroquinone 2 mM. When 4 mM of Cl_3CCOO^- are added to this solution, it becomes yellow, indicating that a hydrogen bonding $QH_2{}^-Cl_3CCOO^-$ complex is formed (Scheme 2B). After addition of 20 mM of HTCA, the solution of Scheme 2B becomes immediately colourless (Scheme 2C), however the yellow colour is spontaneously recovered after 1 h. The loop process indicated in Scheme 2 can be performed an indefinite number of times, which suggests that hydroquinone is never consumed and it acts only as a chemical sensor of an unexpected reaction that involves only the trichloroacetate ion and the respective trichloroacetic acid.

In this framework, the next results were focused on demonstrating the nature of the reaction between the acid and its conjugate base. Thus, it was considered that the mixture of tetrabutylammonium trichloroacetate plus trichloroacetic acid in acetonitrile can be analyzed by cyclic voltammetry. The trichloroacetate ion can be detected through its oxidation wave while the acidic proton of the carboxylic acid can be detected through its respective reduction wave. The oxidation process is generally carried out on glassy carbon electrodes, however, due to the fact that the cathodic reduction of protons is electrocatalyzed on platinum and not on glassy carbon,[9] all the

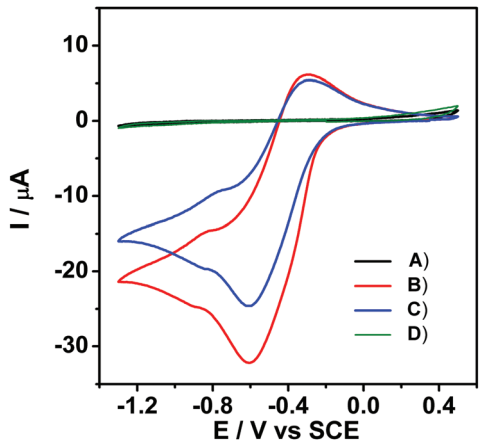

Fig. 2 Cyclic voltammetry in acetonitrile +0.1 M n-Bu_4NPF_6 on a Pt electrode (1 mm ϕ) at 0.1 V s^{-1}. (A) Cl_3CCOO^- 1 mM; (B) Cl_3CCOO^- 1 mM + Cl_3CCOOH 5 mM at t = 0 min; (C) at t = 20 min; (D) at t = 120 min.

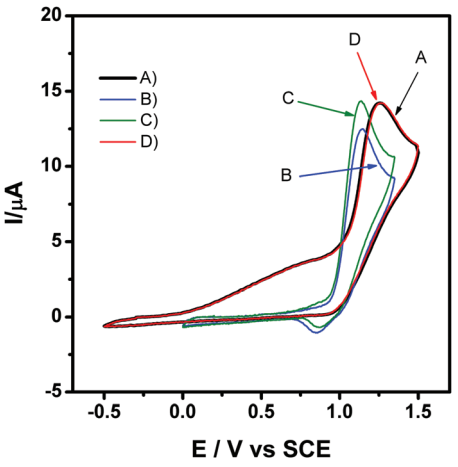

Fig. 3 Cyclic voltammetry in acetonitrile +0.1 M n-Bu_4NPF_6 on a Pt electrode (1 mm ϕ) at 0.1 V s^{-1}. (A) Cl_3CCOO^- 1 mM at t = 0 min; evolution in the time after addition of Cl_3CCOOH 5 mM; (B) t = 20 min, (C) t = 70 min, (D) t = 120 min.

subsequent electrochemical experiments were performed by using this metallic electrode.

Fig. 2A shows the voltammetric behaviour of trichloroacetate ions (1 mM), which is characterized by the lack of any reduction signal, that is, capacitive current is only observed. When trichloroacetic acid is added in excess (5 mM), a single cathodic peak (E_{pc} = −0.6 V/SCE at 0.1 V/SCE), attributed to reduction of acidic protons of the carboxylic acid, is obtained (Fig. 2B). At this stage, the current intensity is a maximum, however, it decreases slowly until the starting capacitive current is recovered after 2 h approximately (Fig. 2C and D). This behaviour is indicative that the carboxylic acid is consumed slowly during the reaction.

In order to know about the behaviour of trichloroacetate ions in the previous mixture, the same experiment was repeated, but in this case by registering the oxidation signal of trichloroacetate ions (Fig. 3).

Fig. 3A corresponds to the initial voltammogram of trichloroacetate oxidation in the absence of trichloroacetic acid, which shows a chemically irreversible anodic peak (E_p = 1.249 V/SCE). Such as was previously analyzed on glassy carbon electrodes for other substituted and non-substituted aliphatic carboxylates,[10] the main peak is related to a non-Kolbe carboxylate oxidation while the prepeak is related to the adsorption of this anion on the platinum electrode.[10a] In the presence of 5 mM of trichloroacetic acid, some features of the voltammogram were modified (Fig. 3B). For example, the main peak was shifted towards less positive values while the prepeak disappearance was observed. Additionally, the peak current intensity was slightly decreased, reaching the minimum value after approximately 20 minutes. After 50 minutes the current intensity is increased (Fig. 3C) and finally the starting voltammogram is recovered after 2 hours (Fig. 3D). Due to the fact that in this experiment the current intensity was in the same order of magnitude, it can be proposed that the concentration of trichloroacetate ions was essentially constant. However, the small difference in current between curve 3A and 3B can be explained in terms of the occurrence of a hydrogen bonding association process between the carboxylate and the carboxylic acid, which yields an association complex $Cl_3CCOO^-\cdots[HOOCCCl_3]_n$ whose stoichiometry could be higher than 1 : 1, probably 1 : 2. Thus, considering the direct proportionality between the peak current and the diffusion coefficient,[11] the decrease in current of voltammogram 3B is explained by the fact that the complex is a more voluminous species that diffuses slowly with respect to the free carboxylate. In agreement with this proposal of association, the blocking of the negative carboxylate function explains also the disappearance of the prewave attributed previously to adsorption of the free anionic carboxylate. With the passage of time, the concentration of carboxylic acid decreases as shown in Fig. 2, and therefore the stoichiometry of the association complex diminishes from 1 : 2 to 1 : 1. In this way, the modification in the association equilibrium results in the increase of the peak current, such as was observed in Fig. 3C. Finally, the original behaviour is recovered after the total consumption of trichloroacetic acid.

From the results described above, it is concluded that trichloroacetic acid and trichloroacetate ion in acetonitrile are involved in a reaction in which the carboxylate concentration remains constant while the concentration of the acid decreases with time.

In order to establish the nature of reaction products and therefore the mechanism, ^1H and ^{13}C NMR experiments in acetonitrile under an argon atmosphere were performed. In this experiment, 3 mL of a concentrated solution of Cl_3CCOOH (0.317 mmol) was mixed under an argon atmosphere with 3 mL of another solution containing 0.322 mmol of tetrabutylammonium trichloroacetate n-$Bu_4N^+Cl_3CCOO^-$. Once the initial Cl_3CCOOH was consumed after 24 h of reaction, 0.224 mmol of Cl_3CCOOH, dissolved in 1.8 mL of deuterated acetonitrile, were also added to increase the concentration of the reaction products. In order to ensure the total consumption of Cl_3CCOOH, the reaction time for this

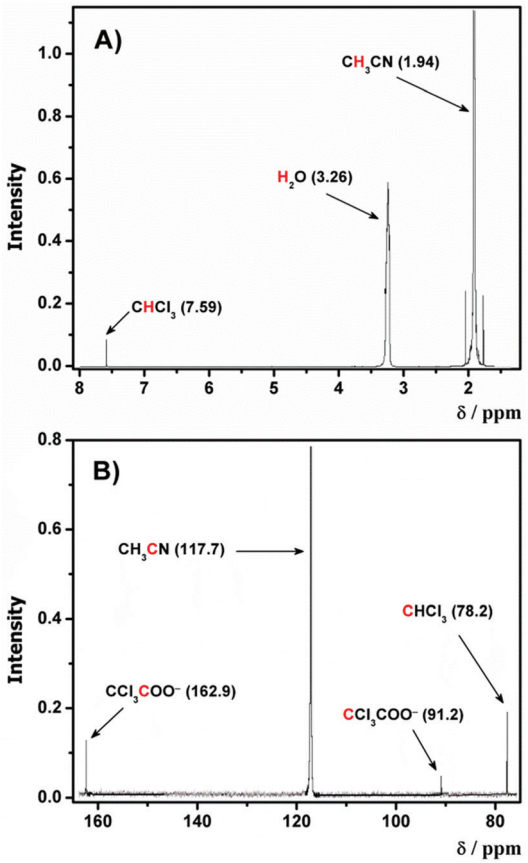

Fig. 4 Nuclear Magnetic Resonance of the mixture of trichloroacetic acid + tetraethylammonium trichloroacetate in deuterated acetonitrile. (A) ^{1}H NMR, (B) ^{13}C NMR.

mixture was about 48 h. After this time, a 150 μL sample of this reaction mixture was placed in an NMR tube containing 450 μL of deuterated acetonitrile.

Fig. 4A shows the ^{1}H NMR spectra, which present the signals corresponding to the hydrogen atoms of acetonitrile (1.94 ppm), water (3.26) and chloroform (7.59 ppm). On the other hand, in the ^{13}C NMR spectra (Fig. 4B), the signal for the carbon atom of acetonitrile (117.7 ppm), trichloroacetate ion (91.2 and 162.9 ppm) and chloroform (78.2 ppm) was obtained.

Due to the presence of chloroform as a product of the reaction between trichloroacetate ions and trichloroacetic acid, the mechanism depicted in Scheme 3 can be proposed.

In this mechanism, the carboxylate and its corresponding conjugate acid generate an association complex ($Cl_3CCOO^{-}\cdots HOOCCCl_3$), which is the precursor of the redox reaction between both species. That is, one electron from the carboxylate Cl_3CCOO^{-} is transferred to the proton of the acid Cl_3CCOOH inside the coordination sphere of the association complex, giving rise to $H^{\cdot}$, the acyloxy radical $Cl_3CCOO^{\cdot}$, and allowing the regeneration of the carboxylate Cl_3CCOO^{-}. Due to the fact that acyloxy radicals are highly unstable,[4] $Cl_3CCOO^{\cdot}$ is rapidly cleaved into CO_2 and the free radical $Cl_3C^{\cdot}$, which can react with $H^{\cdot}$ to generate chloroform Cl_3CH. Although this

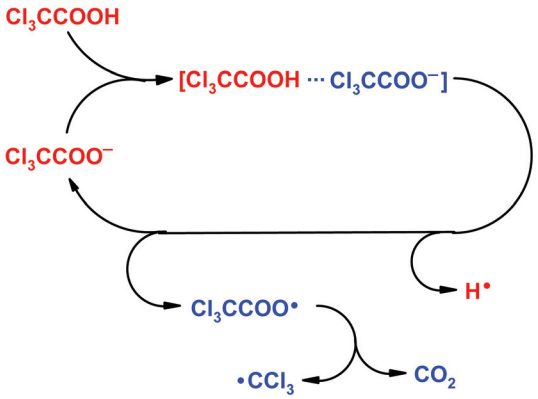

Scheme 3 Redox mechanism of self-decarboxylation.

compound was detected as the sole reaction product, the formation of the radical coupling product Cl_3CCCl_3 cannot be discarded, as it is a volatile gas that could be easily removed during the bubbling of the solutions with argon.

The redox reaction implicit in the loop mechanism depicted in Scheme 3 is equivalent to a self-decarboxylation of trichloroacetic acid redox catalyzed by trichloroacetate ions (eqn (2)), in a global sense. The presence of chloroform as a reaction product as well as the presence of a broad signal at 3450 Gauss in ESR experiments support the proposal that the global self-decomposition mechanism involves in fact radicals (see ESI†).

$$Cl_3CCOOH + Cl_3CCOO^{-} = Cl_3CH + CO_2 + Cl_3CCOO^{-} \quad (2)$$

Another interesting observation about this reaction consists in the fact that by decreasing the number of chlorine atoms in the structures of the acid and carboxylate, the self-decarboxylation tends to be suppressed, which suggests that a high acidity of the acid or a low reduction potential of this one is essential for the occurrence of this phenomenon.

It is worth mentioning that the radical mechanism proposed here contrasts with that assumed in aqueous media, in which the decarboxylation was deemed to be the result of an intramolecular electron transfer from the carboxylate group towards the halogenated moiety.[6a]

In order to know more about the nature of the complex acid-carboxylate that is the precursor of the self-decarboxyl ation process, electronic structure calculations were performed in order to determine the thermochemical viability of reaction (3) as well as that corresponding to eqn (2). Chloroacetic acids–chloroacetate pairs with 1 to 3 chlorine atoms were considered.

$$[Cl_3CCOOH\cdots OOCCCl_3]^{-} = Cl_3CH + CO_2 + Cl_3CCOO^{-} \quad (3)$$

The fully optimized structures of the acid–carboxylate complexes are shown in Fig. 5. It was found that as the number of Cl atoms increases in these species, the distance between the H and the donor O (O^{D}), in the acid fragment, increases. At the same time the distance between the H and the acceptor O (O^{A}), in the anionic fragment, decreases. This indicates that

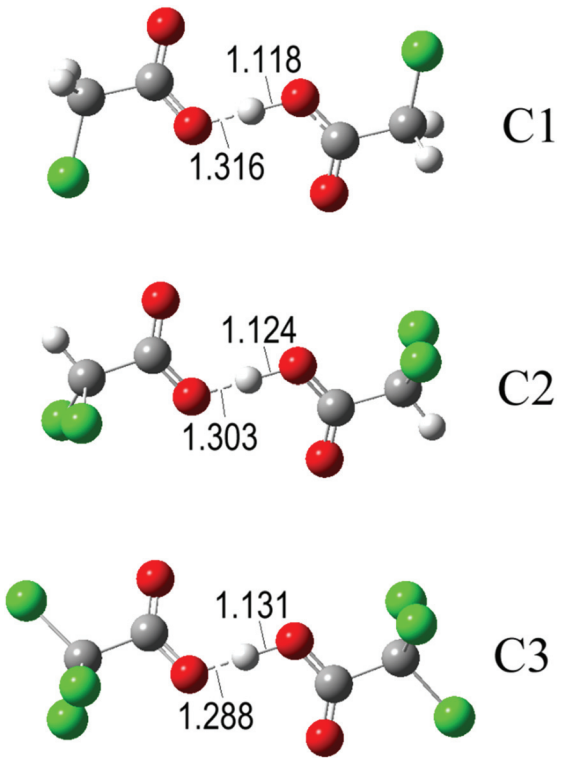

Fig. 5 Fully optimized structures of the Cl_x acetic acids–acetate complexes, with x = 1 to 3. Distances are reported in Å.

Table 1 Electronic charge density ρ and its Laplacian $\nabla^2\rho$, at the bond critical points found for the H donor and the H acceptor sides

	BCP at H donor side		BCP at H acceptor side	
	ρ^{HD}	$\nabla^2\rho^{HD}$	ρ^{HA}	$\nabla^2\rho^{HA}$
C1	0.21206	−0.22863	0.12219	0.00771
C2	0.20806	−0.21518	0.12608	0.00296
C3	0.20283	−0.19673	0.13064	−0.00363

the strength of the hydrogen bonding (HB) increases in the same direction (Cl = 1 < Cl = 2 < Cl = 3).

In order to quantify the strength of the HB interactions leading to the complexes formation, Bader topological analyses[12] of the M05-2X/6-311++G(d,p) wave functions were performed. Two relevant bond critical points (BCPs) were identified in each case, one at the H donor side and the other at the H acceptor side, taking the H atom as reference. Their electronic charge density ρ and its Laplacian, $\nabla^2\rho$, are reported in Table 1. The Laplacian values reported in the table have the opposite sign than those directly produced by the AIM2000 code to facilitate discussion.

The BCPs, which correspond to a maximum of ρ, can also be represented as (3,−1) since they are characterized by two negative values of the Hessian eigenvalues. The values in Table 2 confirm that the critical points found in the present case actually are BCPs. The presence of a BCP at the H acceptor (anion) side confirms the existence of the intermolecular interaction for the studied complexes. Moreover the values of ρ at these BCPs present a clear trend related to the number of chlorine atoms. The ρ values increase with the chlorination degree, which indicates that the strength of the interaction between fragments increases in the same direction. In addition the ρ values corresponding to the BCPs at the H donor side decrease with the chlorination degree, which indicates that the O–H bond in the acid becomes weaker in the complex as the number of chlorine atoms increases. Both behaviors support that the strength of the HB interaction follows the order Cl = 1 < Cl = 2 < Cl = 3.

A more detailed analysis of the BCPs at the donor and at the acceptor sides, based on the Hessian eigenvalues λ_1, λ_2, and λ_3, has also been performed to characterize the nature of the BCPs. It has been established[12] that the value of the ratio $|\lambda_1|/\lambda_3$ allows classifying the interactions. Values of $|\lambda_1|/\lambda_3 > 1$ correspond to shared interactions, like those in covalent bonds; while values of $|\lambda_1|/\lambda_3 < 1$ correspond to closed-shell interactions, such as in H bonds. According to the values in Table 2 it can be established that the $H–O^{HD}$ bond in the acid fragment retains the covalent bond character, while the $H–O^{HA}$ bond involving the acetate is systematically described as closed-shell interactions, in line with the HB interaction between the fragments. Even though this is the case for the three studied complexes, as the chlorination degree increases the covalent character of the $H–O^{HD}$ bond decreases, *i.e.* the $|\lambda_1|/\lambda_3$ becomes closer to 1; while the value of $|\lambda_1|/\lambda_3$ for the $H–O^{HA}$ bond increases. This analysis also supports the order Cl = 1 < Cl = 2 < Cl = 3 for the strength of the interaction between the fragments in the complexes. Negative values of $\nabla^2\rho$ are also characteristic of shared interactions, and positive $\nabla^2\rho$ values are indicative of closed-shell interactions.[12] According to the values in Table 1, the analyses of the $\nabla^2\rho$ values are perfectly congruent with those based on $|\lambda_1|/\lambda_3$ values.

The Gibbs energies of reaction (ΔG) are reported in Table 3, for the global reactions (2) and (3). The ΔG values for the complexation process ($\Delta G^{complex}$) and for the rupture of the radical species (ΔG^{rupt}) are also provided, as well as the adiabatic electron affinities of the acids ($EA^{sol,eA}$) and the adiabatic ionization energies of the anions ($IE^{sol,eD}$), in acetonitrile solution. The thermochemical viability of the complexation process was found to increase with the chlorination degree. The same trend was found for the Gibbs energies of reactions (2) and (3), as well as for the rupture of the radical species. Therefore all the obtained data support that there is a direct relationship between the number of chlorine atoms in the structures of the acid/anion pairs and the facility of the self-decarboxylation process, in agreement with the experimental evidence.

Since the postulated mechanism involves an electron transfer from the carboxylate (electron donor, eD) to the proton of the acid (electron acceptor, eA), the electron affinity of the latter is expected to be significant to the global process, as well as the ionization energies of the acetate ions. The values in Table 3 show that the EA of the acid increases and the IE of the anion decreases with the chlorination degree. Both were in agreement with the trend found for feasibility of the

Table 2 Hessian eigenvalues, at the bond critical points found at the H donor and the H acceptor sides

	BCP at H donor side			BCP at H acceptor side		
	C1	C2	C3	C1	C2	C3
λ_1^{HD}	−0.8623	−0.8366	−0.8113	−0.3427	−0.3615	−0.3836
λ_2^{HD}	−0.8500	−0.8240	−0.7891	−0.3353	−0.3536	−0.3754
λ_3^{HD}	0.7978	0.7999	0.8035	0.7089	0.7269	0.7444
$\lvert\lambda_1\rvert/\lambda_3$	1.08	1.05	1.01	0.48	0.50	0.52

Table 3 Gibbs energies of reaction, in kcal mol^{-1} at 298.15 K, for different processes involving the Cl_x systems (x = 1 to 3), and electron affinities of the acids (eV)

	x = 3	x = 2	x = 1
$\Delta G^{complex}$	−7.36	−7.18	−4.27
$\Delta G^{(2)}$	−19.60	−15.79	−11.39
$\Delta G^{(3)}$	−12.24	−8.61	−7.12
ΔG^{rupt}	−40.09	−32.63	−24.93
$EA^{sol,eA}$	3.98	3.62	3.27
$IE^{sol,eD}$	6.82	6.56	6.24

Table 4 Hirshfeld charges on the atoms involved in the HB (O^{HD}, H, O^{HA}) in the free fragments and in the complexes

	x = 3	x = 2	x = 1
Complex			
O^{HD}	−0.248	−0.256	−0.257
H^{HB}	0.104	0.100	0.095
O^{HA}	−0.292	−0.306	−0.314
Free fragments			
O^{HD}	−0.166	−0.174	−0.179
H^{HB}	0.226	0.219	0.210
O^{HA}	−0.455	−0.472	−0.495

self-decarboxylation process. These trends are shown in Fig. S2 of ESI.†

In addition, a direct relationship has also been found between the ΔG of the self-decarboxylation processes and the ratio between the electronic charge density of the BCP at the H acceptor side and that of the BCP at the H donor side of the complexes (Fig. S3†). This trend suggests that the thermochemical viability of the global self-decarboxylation processes is related to the strength of the postulated complex.

The Hirshfeld charges on the atoms involved in the formation of the H bonded complex are reported in Table 4. These atoms are the oxygen atom in the acid fragment acting as the H donor (O^{HD}), the H atom involved in the HB interaction (H^{HB}), and the oxygen atom in the acetate fragment acting as the H acceptor (O^{HA}). According to the values in this table the positive charge of the H atom is significantly lower in the complex, compared to that in the isolated acid. In addition the charge on the O atom in the acetate fragment becomes less negative in the complex, while that on the O atom (directly bonded to the H) in the acid becomes more negative, also compared to the isolated fragments. These results support the postulated electron transfer between the acid and carboxylate fragments in the association complex.

Conclusions

The self-decarboxylation process occurs in mixtures of trichloroacetic acid with tetraethylammonium trichloroacetate in acetonitrile. This reaction involves the formation of a hydrogen bonding association complex, which promotes intramolecular one-electron exchange. In this reaction, the carboxylate lost an electron, giving rise to a highly unstable acyloxy radical which is rapidly decomposed into carbon dioxide and the trichloromethyl radical. The electron lost by the carboxylate is used to reduce the acidic proton of the trichloroacetic acid, allowing formation of monoatomic hydrogen and the regeneration of the carboxylate. Although the coupling of trichloromethyl radicals is possible, the sole reaction product detected was chloroform, which is the result of the reaction between the trichloromethyl radical and the monoatomic hydrogen. The equivalent reactions with mixtures of acetate–acetic acid and chloroacetate–chloroacetic acid were not possible, allowing us to conclude that the self-decarboxylation mechanism is possible because of the high acidity of the easily reducible proton of trichloroacetic acid. Hydroquinone is a good molecular sensor of this reaction because it permits one to observe the regeneration of the carboxylate by forming an ionic-neutral hydrogen bonding yellow complex.

Electronic structure calculations revealed that the strength of the interaction between fragments increases with the degree of chlorination. The low value of positive charge on the H atom in the acid fragment of the complex as well as the low value of negative charge on the O atom in the complementary acetate fragment, with respect to the respective free species, support the intramolecular electron transfer that activates the self-decarboxylation mechanism. In agreement with this, the energies of complex formation and complex cleavage indicate that the global self-decarboxylation processes are also thermochemically more favourable with the chlorination degree.

Experimental

Chemicals

Acetonitrile HPLC, distilled over phosphorous pentoxide, was used as the solvent. Tetrabutylammonium hexafluorophosphate (98%) (n-Bu_4NPF_6), crystallized from ethanol, was the

supporting electrolyte. The tetrabutylammonium trichloroacetate was prepared in dry methanol in a Schlenck tube by mixing stoichiometric amounts of trichloroacetic acid (99%) and tetrabutylammonium hydroxide 1 M–methanol. The water produced in this reaction was eliminated under vacuum as a water–methanol azeotrope.

Electrochemical instrumentation and electrodes

The electrochemical apparatus consisted in a potentiostat DEA-332 (Radiometer Copenhagen) with positive feedback resistance compensation. A conventional three electrode cell was used to carry out the voltammetric experiments. The working electrode was a 1 mm diameter platinum disk, which was polished with 0.3 μm alumina powder and ultrasonically rinsed with distilled water and ethanol before each experimental run. The auxiliary electrode was a platinum mesh and the reference electrode a Saturated Calomel Electrode (SCE). A salt bridge containing 0.1 M n-$Bu_4NPF_6^+$ acetonitrile solution connected the cell with the reference electrode. All the electrochemical experiments were performed at room temperature (~25 °C).

Spectroscopic instrumentation

^1H and ^{13}C NMR spectra were recorded on a JEOL EKA-500 spectrometer. X-band ESR spectra were collected using an EMX Plus Bruker System and by using a Wilmad cell. The samples were prepared under an argon atmosphere, in deuterated acetonitrile. In all the cases, the experiments were performed at room temperature.

Computational details

All the electronic calculations were performed with the Gaussian 09 package of programs.[13] Geometry optimizations and frequency calculations were carried out using the M05-2X functional[14] and the 6-311++G(d,p) basis set. They have been carried out in solution, using the SMD continuum model[15] and acetonitrile as the solvent. The M05-2X functional has been chosen for the task at hand because it has been proven to be among the functionals with the best performance for general purpose applications in thermochemistry, kinetics, and noncovalent interactions involving nonmetals.[12] It is also among the best performing functionals for calculating reaction energies involving free radicals.[16] The SMD solvent model has been chosen since its performance for describing solvation in energies of both neutral and ionic species, in aqueous and also in non-aqueous solvents, is better than that achieved with other solvent models. Geometries were fully optimized without imposing any restriction. Local minima were confirmed by the absence of imaginary frequencies. Thermodynamic corrections at 298.15 K were included in the calculation of relative energies. The Bader topological analyses[12] of the wave functions were performed with the AIM2000 code.[17]

Acknowledgements

D.P.V. and P.D.A.S. acknowledge Conacyt for a PhD grant. The authors acknowledge B.R. Díaz and L.S. Hernández for their assistance with the acquisition of the NMR and ESR spectra. The authors acknowledge CONACyT for financial support through the project 103714.

Notes and references

1 (*a*) Y. Matsumura, *Encyclopedia of Electrochemistry*, Wiley-VCH, 2007, ch. 6, vol. 8003B; (*b*) H. J. Shaefer, *Top. Curr. Chem.*, 1990, **152**, 90; (*c*) J. H. P. Utley, *Technics in Electroorganic Synthesis*, Wiley, 1974, Part I, vol. 5; (*d*) A. K. Vijh and B. E. Conway, *Chem. Rev.*, 1967, **67**, 623; (*e*) S. Torii and H. Tanaka, *Organic Electrochemistry*, Marcel Dekker, New York, 2001, ch. 14.

2 (*a*) C. P. Andrieux, F. González and J.-M. Savéant, *J. Am. Chem. Soc.*, 1997, **119**, 4292; (*b*) P. A. Brooksby, A. J. Downard and S. S. C. Yu, *Langmuir*, 2005, **21**, 11304; (*c*) F. Geneste, M. Cadoret, C. Moinet and G. Jezequel, *New J. Chem.*, 2002, **26**, 1261; (*d*) L. B. Venarusso, K. Tammeveski and G. Maia, *Electrochim. Acta*, 2011, **15**, 1535; (*e*) L. S. Hernández-Muñoz, M. A. González-Fuentes, B. R. Díaz, R. Fragoso, C. Vázquez-López and F. J. González, *Electrochim. Acta*, 2012, **63**, 287.

3 (*a*) C. P. Andrieux, F. González and J.-M. Savéant, *J. Electroanal. Chem.*, 2001, **498**, 171; (*b*) A. A. Isse, A. Gennaro and F. Maran, *Acta Chem. Scand.*, 1999, **53**, 1013.

4 (*a*) J. W. Hilborn and J. A. Pincock, *J. Am. Chem. Soc.*, 1991, **113**, 2683; (*b*) T. M. Bockman, S. M. Hubig and J. K. Kochi, *J. Am. Chem. Soc.*, 1996, **118**, 4502; (*c*) T. M. Bockman, S. M. Hubig and J. K. Kochi, *J. Org. Chem.*, 1997, **62**, 2210.

5 (*a*) S. E. Treimer and D. H. Evans, *J. Electroanal. Chem.*, 1998, **455**, 19; (*b*) S. E. Treimer and D. H. Evans, *J. Electroanal. Chem.*, 1998, **449**, 39.

6 (*a*) X. Zhang and R. A. Minear, *Water Res.*, 2002, **36**, 3665; (*b*) L. Heller-Grossman, J. Manka, B. Limoni-Relis and M. Rebhun, *Water Res.*, 1993, **27**, 1323.

7 (*a*) J. Q. Chambers, *Electrochemistry of Quinones in The Chemistry of Quinonoid Compounds*, ed. S. Patai and Z. Rappaport, Wiley, 1988, ch. 12, vol. II; (*b*) M. Aguilar, N. Macías, J. A. Bautista, M. Gómez, F. J. González and I. González, *Curr. Org. Chem.*, 2004, **8**, 1721; (*c*) P. S. Guin, S. Das and P. C. Mandal, *Int. J. Electrochem. Sci.*, 2012, 1–22.

8 P. D. Astudillo, J. Tiburcio and F. J. González, *J. Electroanal. Chem.*, 2007, **604**, 57.

9 (*a*) E. Santos, P. Quaino and W. Schmickler, *Phys. Chem. Chem. Phys.*, 2012, **14**, 11224; (*b*) S. Trasatti, *J. Electroanal. Chem.*, 1972, **39**, 163.

10 (*a*) M. Galicia and F. J. González, *J. Electrochem. Soc.*, 2002, **149**, 46; (*b*) M. Galicia, M. A. González-Fuentes, D. P. Valencia and F. J. González, *J. Electroanal. Chem.*,

2012, **672**, 28; (*c*) J. M. Kornprobst, A. Laurent and E. Laurent-Dieuzeide, *Bull. Soc. Chim. Fr.*, 1968, **9**, 3657.
11 (*a*) D. P. Valencia and F. J. González, *J. Electroanal. Chem.*, 2012, **681**, 121; (*b*) D. P. Valencia and F. J. González, *Electrochem. Commun.*, 2011, **13**, 129; (*c*) T. Matsue, D. H. Evans, T. Osa and N. Kobayashi, *J. Am. Chem. Soc.*, 1985, **107**, 3411.
12 R. F. W. Bader, *Atoms in Molecules – A Quantum Theory*, Oxford University Press, Oxford, 1990.
13 M. J. Frisch, G. W. Trucks, H. B. Schlegel, G. E. Scuseria, M. A. Robb, J. R. Cheeseman, G. Scalmani, V. Barone, B. Mennucci, G. A. Petersson *et al. GAUSSIAN 09 (Revision A.08)*, Gaussian Inc., Wallingford CT, 2009.
14 Y. Zhao, N. E. Schultz and D. G. Truhlar, *J. Chem. Theory Comput.*, 2006, **2**, 364.
15 A. V. Marenich, C. J. Cramer and D. G. Truhlar, *J. Phys. Chem. B*, 2009, **113**, 6378.
16 Y. Zhao and D. G. Truhlar, *J. Phys. Chem. A*, 2008, **112**, 1095.
17 F. Biegler-Köning, *AIM2000, Version 1 0*, University of Applied Sciences, Bielefeld, Germany, 2000.